Data in Brief 19 (2018) 665–677

Contents lists available at ScienceDirect

Data in Brief

journal homepage: www.elsevier.com/locate/dib

Data Article

Characterization of the synthetic biology-inspired implementation of a materials-based positive feedback loop

Hanna J. Wagner [a,b,c], Raphael Engesser [c,d], Kathrin Ermes [a,c], Christian Geraths [a,c], Jens Timmer [c,d], Wilfried Weber [a,b,c,*]

[a] Faculty of Biology, University of Freiburg, Schänzlestrasse 1, 79104 Freiburg, Germany
[b] Spemann Graduate School of Biology and Medicine (SGBM), University of Freiburg, Albertstrasse 19a, 79100 Freiburg, Germany
[c] BIOSS - Centre for Biological Signalling Studies, University of Freiburg, Schänzlestrasse 18, 79104 Freiburg, Germany
[d] Institute of Physics, University of Freiburg, Hermann-Herder Strasse 3, 79104 Freiburg, Germany

ARTICLE INFO

Article history:
Received 27 April 2018
Accepted 15 May 2018
Available online 18 May 2018

Keywords:
Information-processing
Protease
Signal amplification
Smart materials
Stimulus-responsive

ABSTRACT

The translation of engineering designs to materials sciences by means of synthetic biological tools represents a novel concept for the development of information-processing materials systems. Here, we provide data on the mathematical model-guided implementation of a biomaterials-based positive feedback loop for the detection of proteolytic activities. Furthermore, we present data on an extended system design for the detection of the antibiotic novobiocin.

This work is related to the research article "Synthetic biology-inspired design of signal-amplifying materials systems" (Wagner et al., 2018) [1].

DOI of original article: https://doi.org/10.1016/j.mattod.2018.04.006
* Corresponding author at: Faculty of Biology, University of Freiburg, Schänzlestrasse 1, 79104 Freiburg, Germany.
E-mail address: wilfried.weber@biologie.uni-freiburg.de (W. Weber).

https://doi.org/10.1016/j.dib.2018.05.074

Specifications Table

Subject area	*Biology, Biomaterials*
More specific subject area	*Synthetic biology, Materials systems*
Type of data	*Figures, graphs, images, tables*
How data was acquired	*Fluorescence measurements (*Infinite M200 pro microplate reader, Tecan), SDS-PAGE image digitization (ImageQuant LAS 4000, GE Healthcare)
Data format	*Analyzed*
Experimental factors	*The system response was monitored over time; samples were collected at different points in time and stored at RT until measuring the fluorescence of all samples.*
Experimental features	*Materials were functionalized with engineered proteins and assembled in a positive feedback loop configuration. The system behavior in response to different inducer concentrations was monitored by measuring the dissolution of an output material by determining the release of the incorporated fluorescent protein mCherry.*
Data source location	*This work was done at the University of Freiburg, Germany.*
Data accessibility	*Raw / processed data are available from Mendeley Data.*

Value of the data

- The herein presented data represent an example of the translation of synthetic biological tools to polymer materials for the construction of information-processing materials systems and could serve as blueprint for the development of further such systems for different applications.
- The generation of materials systems by a mathematical model-guided approach might be a generic strategy for the design and optimization of information-processing materials systems.
- All system components are modular and interchangeable, which offers the possibility to deploy other polymers, functionalities, and proteins for the development of novel systems with desired functions.

1. Data

The model scheme of the materials-based positive feedback loop and profile-likelihood of estimated model parameters are shown in Fig. 1. The corresponding estimated parameters are summarized in Table 1. Fig. 2 shows the data and model fits of the positive feedback loop system at different Caspase-3 (Casp3) and inducer concentrations. The Tobacco etch virus (TEV) protease fusion construct was modified to enable a direct 3C protease (3CPRO)-mediated release of TEV and thus a forward amplification (Fig. 3). The data of the resulting system with either sole forward or combined forward and feedback loop amplification at different TEV, Casp3 and 3CPRO inducer concentrations are shown in Fig. 4. Table 2 presents the mathematical validation of the combined materials system.

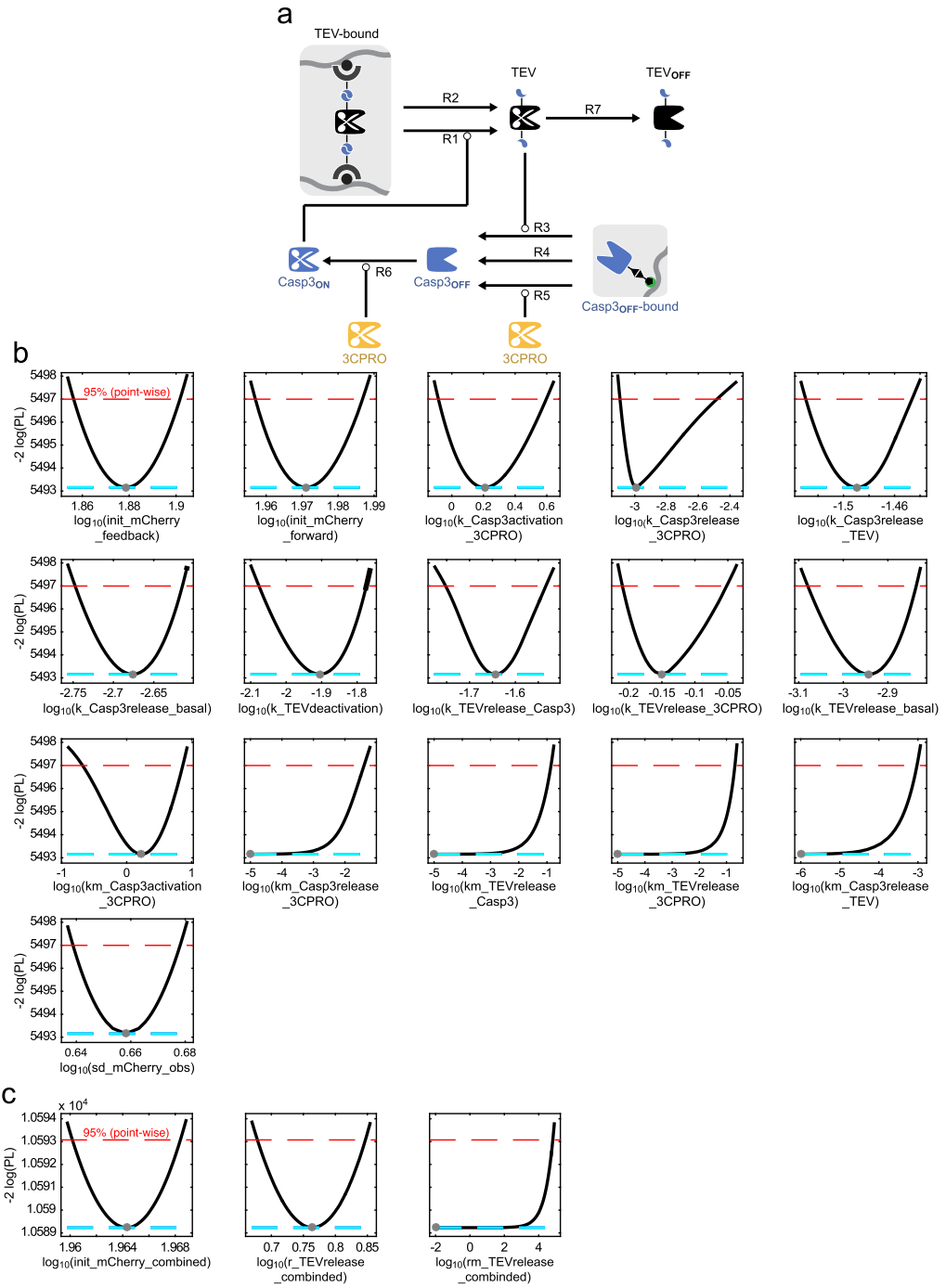

Fig. 1. Model scheme and profile likelihood of the estimated parameters of the signal-amplifying materials system. **(a)** Core model of the system. The K_d-dependent basal release of TEV protease and Casp3 from the materials is indicated by arrows R2 and R4. Released TEV protease enhances the release of non-active Casp3 (R3). Additionally, 3CPRO is able to cleave the TCS linker thereby contributing to the release of Casp3 (R5). Released Casp3 is cleaved and activated by 3CPRO (R6). Active Casp3 cuts the CCS linker of the TEV construct, thus enhancing TEV protease release and closing the feedback loop. The enzymatic activity of TEV protease decreases over time as indicated by reaction R7. **(b)** Profile likelihood of the estimated parameters of the basic feedback and forward amplification system (corresponding to Fig. 4a, c in Ref. [1]). **(c)** Profile likelihood of the estimated parameters of the combined system (corresponding to Fig. 4f in Ref. [1]). (b, c) The solid lines indicate the profile likelihood, the optimal parameter set is marked with a grey star. The red dashed line marks the 95% confidence level. The light blue dashed line indicates the −2 log(PL) value of the optimal parameter set. The parameter axis is on a logarithmic scale.

Table 1
Estimated parameters of the positive feedback material. Fitted parameter values obtained by maximum likelihood estimation. σ^- and σ^+ indicate the 95% point-wise confidence intervals calculated by exploring the profile likelihood.

Parameter	$\hat{\theta}$	σ^-	σ^+	Unit
$k_{TEVrelease,CASP3}$	$2.27 \cdot 10^{-02}$	$1.77 \cdot 10^{-02}$	$2.93 \cdot 10^{-02}$	$mU^{-1}\ h^{-1}$
$k_{TEVrelease,basal}$	$1.14 \cdot 10^{-03}$	$8.32 \cdot 10^{-04}$	$1.46 \cdot 10^{-03}$	h^{-1}
$k_{TEVrelease,3CPRO}$	$7.07 \cdot 10^{-01}$	$6.17 \cdot 10^{-01}$	$8.87 \cdot 10^{-01}$	$\mu g^{-1}\ mL\ h^{-1}$
$k_{TEVdeactivation}$	$1.24 \cdot 10^{-02}$	$8.38 \cdot 10^{-03}$	$1.68 \cdot 10^{-02}$	h^{-1}
$k_{Casp3release,TEV}$	$3.24 \cdot 10^{-02}$	$2.95 \cdot 10^{-02}$	$3.58 \cdot 10^{-02}$	$RU^{-1}\ h^{-1}$
$k_{Casp3release,basal}$	$2.11 \cdot 10^{-03}$	$1.79 \cdot 10^{-03}$	$2.43 \cdot 10^{-03}$	h^{-1}
$k_{Casp3release,3CPRO}$	$1.01 \cdot 10^{-03}$	$8.07 \cdot 10^{-04}$	$3.29 \cdot 10^{-03}$	$\mu g^{-1}\ mL\ h^{-1}$
$k_{Casp3activation,3CPRO}$	$1.61 \cdot 10^{+00}$	$8.23 \cdot 10^{-01}$	$3.95 \cdot 10^{+00}$	$\mu g^{-1}\ mL\ h^{-1}$
$k_{m,Casp3activation,3CPRO}$	$1.70 \cdot 10^{+00}$	$2.09 \cdot 10^{-01}$	$7.32 \cdot 10^{+00}$	mU^{-1}
$k_{m,Casp3release,3CPRO}$	0	0	$4.05 \cdot 10^{-02}$	mU^{-1}
$k_{m,TEVrelease,CASP3}$	0	0	$1.39 \cdot 10^{-01}$	RU^{-1}
$k_{m,TEVrelease,3CPRO}$	0	0	$2.04 \cdot 10^{-01}$	RU^{-1}
$k_{m,Casp3release,TEV}$	0	0	$9.43 \cdot 10^{-04}$	mU^{-1}
$init_{mCherry,feedback}$	$7.56 \cdot 10^{+01}$	$7.18 \cdot 10^{+01}$	$7.97 \cdot 10^{+01}$	%
$init_{mCherry,forward}$	$9.36 \cdot 10^{+01}$	$9.06 \cdot 10^{+01}$	$9.70 \cdot 10^{+01}$	%
$sd_{mCherry,obs}$	$4.55 \cdot 10^{+00}$	$4.35 \cdot 10^{+00}$	$4.77 \cdot 10^{+00}$	%

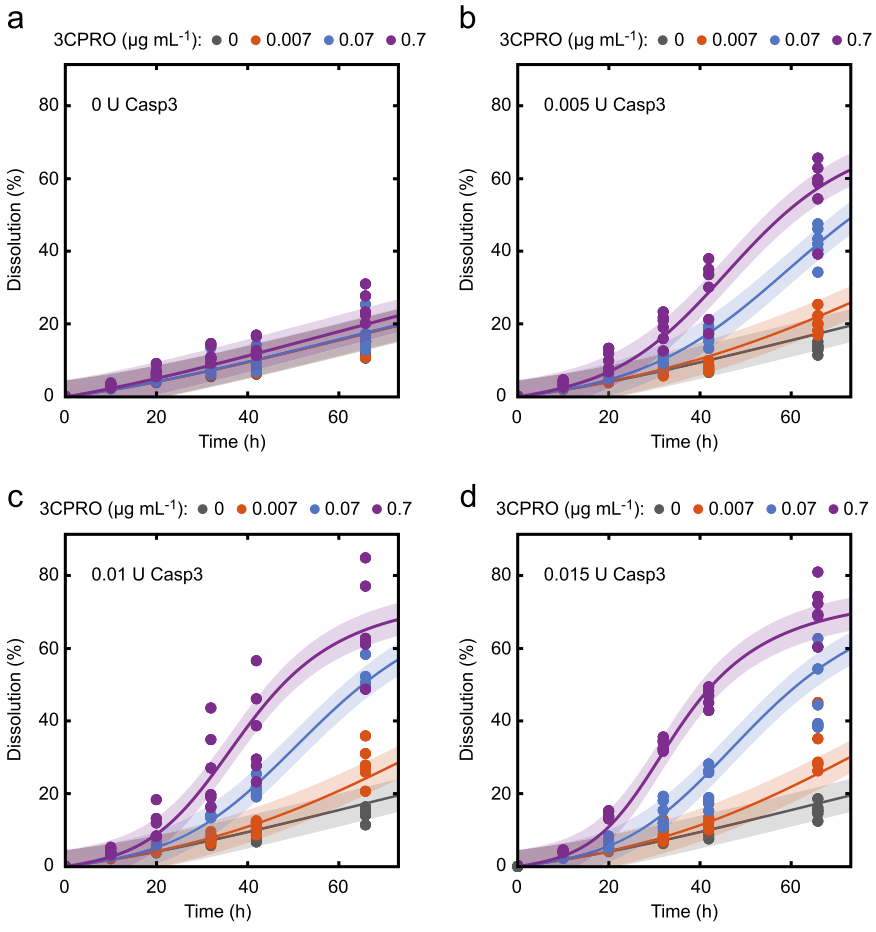

Fig. 2. Assembly and characterization of the basic signal-amplifying materials system. Hydrogels (module B) were synthesized with 0 **(a)**, 0.005 U **(b)**, 0.01 U **(c)** or 0.015 U **(d)** Casp3 and combined with material module A (2.0 RU TEV protease). The indicated amounts of 3CPRO were added and the dissolution of the output hydrogel was monitored by quantifying the fluorescence of released mCherry. The curves represent the model fits. The shaded error bands correspond to one standard deviation. d taken from Ref. [1].

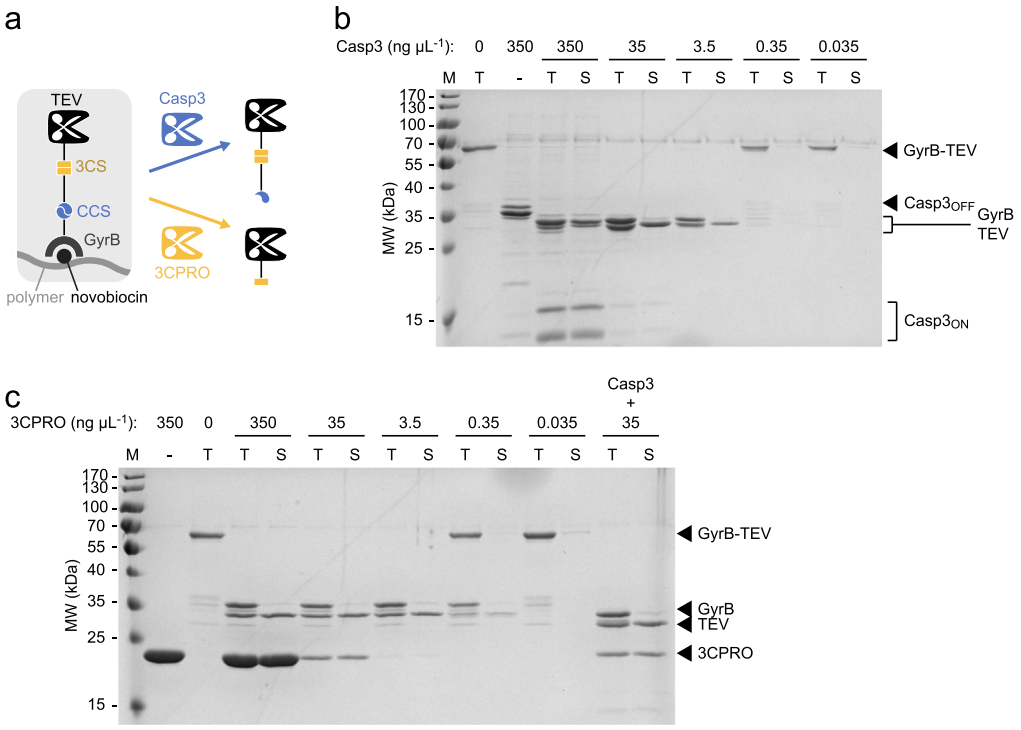

Fig. 3. Adaption of the module A for a signal-amplifying materials system with faster response characteristics (forward amplification) and increased sensitivity (combined forward and feedback amplification). **(a)** Design of a TEV protease construct that can be immobilized on a novobiocin-functionalized material via a GyrB domain and released by cleavage of the 3CPRO cleavage site (3CS, forward amplification) or Casp3 cleavage site (CCS, positive feedback). **(b, c)** Characterization of TEV release from material module A (Fig. 4c, f in Ref. [1]) by 3CPRO (b) or Casp3 (c). 80 µg TEV protease were incubated with 8 µL novobiocin-agarose in a total volume of 33 µL hydrogel buffer at 4 °C overnight. The material was washed with hydrogel buffer and combined with the indicated concentrations of Casp3 (b), 3CPRO (c), or both proteases (last two lanes in c, 35 ng µL^{-1} Casp3) in a total volume of 100 µL hydrogel buffer. The samples were incubated at 4 °C overnight and released (S, supernatant) as well as total (T) protein was analyzed by SDS-PAGE.

The system design was extended for the detection of novobiocin and assembled in forward and combined forward and feedback loop configurations. The response at different TEV, Casp3, 3CPRO and novobiocin concentrations was monitored (Fig. 5). Fig. 6 provides data on the degree of functionalization of the novobiocin-functionalized material. Tables 3 and 4 summarize the cloning of all plasmids and primers used in this study.

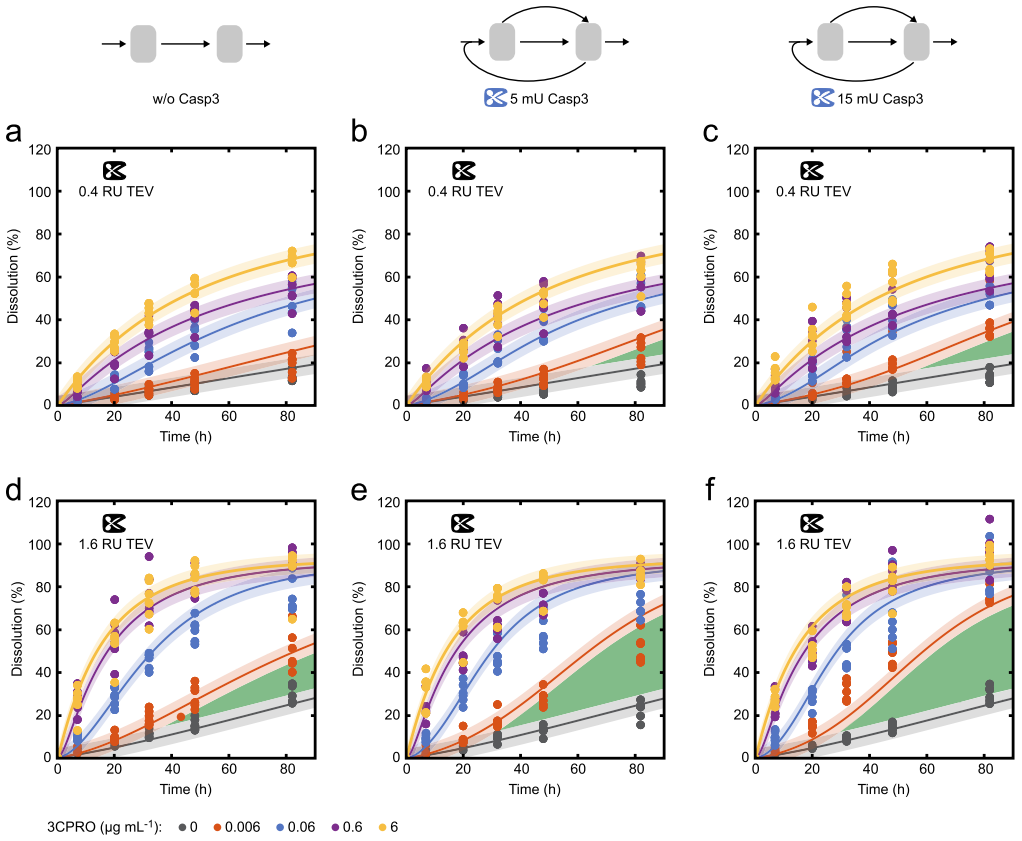

Fig. 4. Experimental implementation of optimized two-materials-based signal-amplifying materials systems. Hydrogels (module B) were synthesized with 0 U **(a, d)**, 0.005 U **(b, e)**, or 0.015 U **(c, f)** Casp3 and combined with module A (containing 0.4 RU (a-c) or 1.6 RU (d-f) TEV protease). The indicated concentrations of 3CPRO were added and the dissolution of module B was monitored by quantifying the fluorescence of released mCherry. The curves represent the model fits. The shaded error bands correspond to one standard deviation. d,f taken from Ref. [1].

Table 2
Validation of the positive feedback material. Fitted parameter values of the additional parameters in the validation with the combined feedback material (see Fig. 4f in Ref. [1]) obtained by maximum likelihood estimation. σ^- and σ^+ indicate the 95% point-wise confidence intervals calculated by exploring the profile likelihood.

Parameter	$\hat{\theta}$	σ^-	σ^+	Unit
$r_{TEVrelease,combined}$	$9.21 \cdot 10^{+00}$	$9.12 \cdot 10^{+00}$	$9.30 \cdot 10^{+00}$	1
$r_{m,TEVrelease,combined}$	0	0	$6.60 \cdot 10^{+04}$	1
$init_{mCherry,combined}$	$9.21 \cdot 10^{+01}$	$9.12 \cdot 10^{+01}$	$9.30 \cdot 10^{+01}$	%

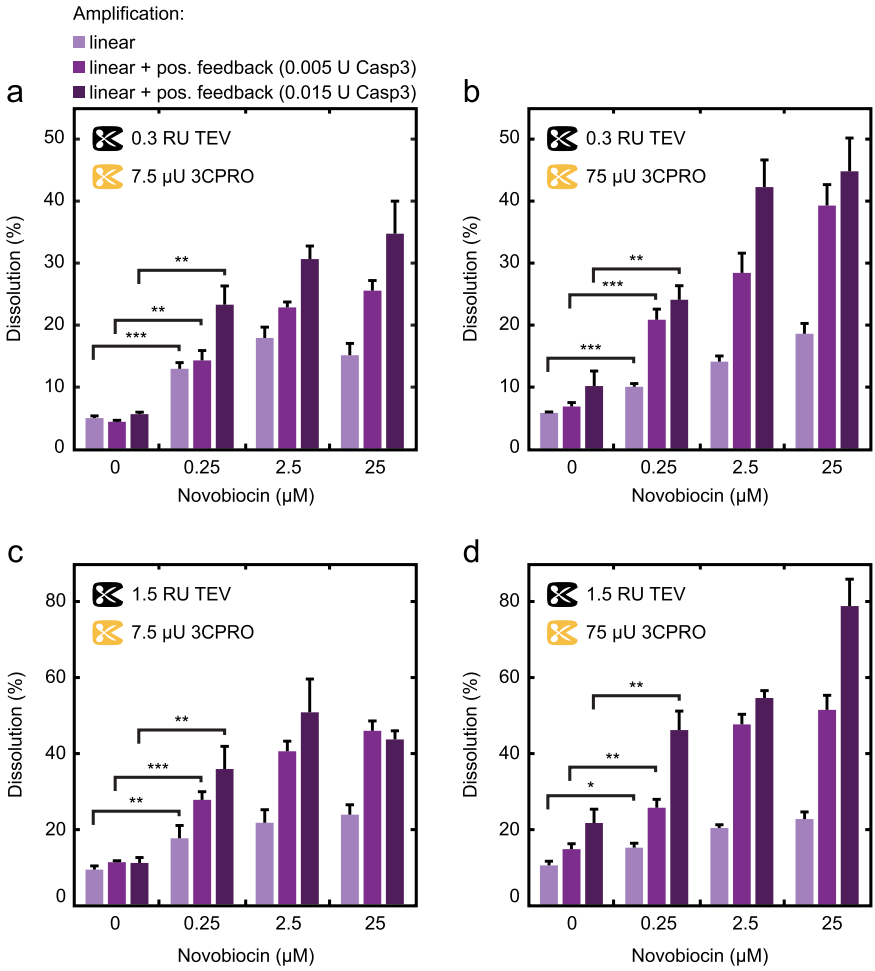

Fig. 5. Assembly and characterization of the signal-amplifying materials system for the detection of novobiocin. Hydrogels (module B) were synthesized with 0 U, 0.005 U, or 0.015 U Casp3. They were combined with material module A comprising 0.3 RU **(a, b)** or 1.5 RU **(c, d)** TEV, and with the 3CPRO-containing material loaded with 7.5 µU **(a, c)** or 75 µU **(b, d)** 3CPRO. The resulting three modules-comprising materials system was incubated with the indicated concentrations of novobiocin and the dissolution of the output hydrogels (module B) was monitored by determining the mCherry fluorescence in the supernatants. Mean values of at least five replicates +/- s.e.m. after 49 h are shown. Statistical analysis: unpaired t-test with Welch's correction, $^{*}p < 0.05$, $^{**}p < 0.01$, $^{***}p < 0.001$. c adapted from Ref. [1].

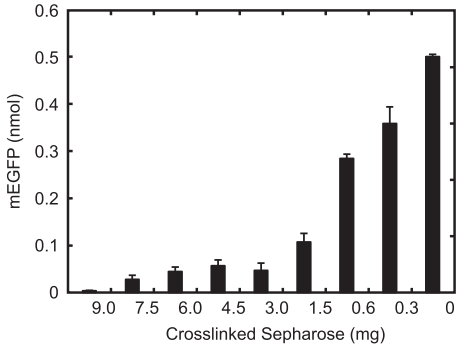

Fig. 6. Determination of the binding capacity of novobiocin-functionalized Sepharose. After functionalizing the indicated amounts of crosslinked Sepharose with novobiocin, the material was incubated with 0.5 nmol GyrB-mEGFP-3CPRO at 4 °C for 7.5 h, rotating. Unbound protein was quantified by measuring the fluorescence of mEGFP in the supernatant. Mean values of four replicates +/- s.e.m. are shown.

Table 3
Plasmids used for the signal-amplifying materials system.

Plasmid	Description	Reference	Used for
pHB325	P_{SV40}-Casp3(Tev-S2)-pA Mammalian expression vector for TEV protease-inducible Casp3.	Casp3(Tev-S2) sequence taken from Gray et al. [2]	Cloning of pHJW186.
pHJW1	P_{T7}-Casp3-TCS-His_6 One backbone half of pKJ57 was PCR amplified using oligonucleotides oHJW1 and oHJW5; the second backbone half including the Casp3 gene was amplified from pKJ57 using oHJW2 and oHJW6; TCS-linker sequence was amplified from pKJ60 using oHJW3 and oHJW4 - all three fragments were assembled by Gibson cloning [3].	This work	Cloning of pHJW181.
pHJW2	P_{T7}-His_6-TCS-mCherry-TCS-His_6 His_6-TCS was PCR amplified from pKJ60 using oligonucleotides oHJW7 and oHJW8; mCherry was amplified from pKJ10 using oHJW9 and oHJW10; TCS-linker was amplified from pKJ60 using oHJW11 and oHJW12; the backbone was amplified in two halves from pKJ60 using oHJW1 and oHJW5, and oHJW6 and oHJW13. All five fragments were assembled by Gibson cloning.	This work	Synthesis of crosslinker for material module B.
pHJW3	P_{T7}-His_6-3CS-GyrB-TEV Oligonucleotides oHJW14 and oHJW15 were annealed and ligated into pKJ39 (*Eco*RI/*Xho*I/*Sph*I, three fragment ligation) thereby replacing the His_6-tag sequence with the His_6-3CS sequence.	This work	Characterization of material module B depicted in Fig. 3b in Ref. [1]. Prior to its use, the His_6-tag was removed from the protein using 3CPRO (HJW4).
pHJW4	P_{T7}-His_6-3CPRO The coding sequence for the human rhinovirus type 14 3C protease (GenBank accession no. https://www.ncbi.nlm.nih.gov/nuccore/K02121) was codon-optimized for expression in *E. coli* and ordered as gene synthesis (Life Technology). The gene was cloned into pKJ10 (*Hind*III/*Nde*I) thereby replacing the His_6-mCherry coding sequence.	This work	Used for cloning of pHJW183, activation of Casp3 (Fig. 2b in Ref. [1]), and removal of His_6-tag from HJW3.
pHJW53	P_{T7}-His_6-3CS-GyrB-CCS-TEV-CCS-GyrB His_6-3CS-GyrB-CCS-TEV-CCS was PCR amplified from pHJW3 using oligonucleotides oHJW136 and oHJW141. C-terminal GyrB was amplified from pHJW3 using oHJW142 and oHJW143. The backbone of pHJW2 was amplified using oHJW1 and oHJW13. All fragments were assembled by Gibson cloning.	This work	Basic feedback loop and novobiocin-detecting materials systems (Figs. 4b and 5d, f in Ref. [1], Figs. 2 and 5).
pHJW177	P_{T7}-His_6-GyrB-CCS-3CS-TEV The coding sequence for TEV protease was PCR amplified from pHJW3 using oligonucleotides oHJW483 and oHJW141. His_6-GyrB-CCS-3CS was amplified from pKJ39 using oHJW484 and oHJW431. Backbone fragments were amplified from pHJW3 using oHJW485 and oHJW143, and oHJW1 and oHJW205. All fragments were assembled by Gibson cloning.	This work	Forward amplification and combined materials systems (Fig. 4e, h in Ref. [1] Figs. 3 and 4).
pHJW181	P_{T7}-Casp3($3CPRO_{ind}$)-TCS-His_6	This work	Characterization of material module A (Fig. 2b in Ref. [1]). Incorporation into

Table 3 (*continued*)

Plasmid	Description	Reference	Used for
	The 3CS was inserted into pHJW1 by PCR amplification of pHJW1 using oligonucleotides oHJW421 and oHJW5, and oHJW422 and oHJW6. oHJW421 and oHJW422 contained the 3CS sequence in their overhangs. Both fragments were assembled by Gibson cloning.		module B (Fig. 4b, h and 5 f in Ref. [1], Figs. 2, 4 and 5).
pHJW183	P_{T7}-His_6-GyrB-mEGFP-3CPRO The mEGFP sequence was PCR amplified from pMH175 using oligonucleotides oHJW427 and oHJW428. 3C protease including one half of the backbone was amplified from pHJW4 using oHJW429 and oHJW5. His_6-GyrB was amplified from pKJ39 using oHJW430 and oHJW431. The second half of the backbone was amplified from pHJW4 using oHJW6 and oHJW205. All fragments were assembled by Gibson cloning.	This work	Determination of binding capacity of novobiocin-Sepharose (Fig. 6), and extended materials system for the detection of novobiocin (Fig. 5f in Ref. [1], Fig. 5).
pHJW186	P_{T7}-Casp3(TEV_{ind})-TCS-His_6TEV-cleavable Casp3 was amplified from pHB325 using oligonucleotides oKJ136 and oHJW2. TCS-His6 and one half of the backbone was amplified from pHJW1 using oHJW3 and oHJW5. The second half of the backbone was amplified from pHJW181 using oHJW6 and oKJ129. All fragments were assembled by Gibson cloning.		Characterization of adapted material module A for combined forward and feedback amplification, depicted in Fig. 3.
pHJW199	P_{T7}-His_6-GyrB-CCS-TEV-CCS-GyrB His_6-GyrB-CCS-5'TEVwas excised from pKJ39 (*Nde*I) and ligated with pHJW53 (*Nde*I).		Characterization of material module A (Fig. 2b in Ref. [1]).
pKJ10	P_{T7}-His_6-mCherry Bacterial expression vector encoding hexahistidine-tagged mCherry.	Unpublished	Cloning of pHJW2.
pKJ39	P_{T7}-His_6-GyrB-CCS-TEV Bacterial expression vector encoding hexahistidine-tagged GyrB-TEV fusion protein.	Unpublished	Cloning of pHJW3, pHJW177 and pHJW183.
pKJ57	P_{T7}-Casp3-His_6 Bacterial expression vector encoding hexahistidine-tagged Caspase-3.	Unpublished	Cloning of pHJW1.
pKJ60	P_{T7}-His_6-TCS-F_M Bacterial expression vector encoding hexahistidine-tagged F36M variant of human FK-binding protein 12 (F_M).	Unpublished	Cloning of pHJW1 and pHJW2.
pMH175	P_{T7}-mEGFP-PIF3(1–100)-His_6 Bacterial expression vector encoding hexahistidine-tagged mEGFP-PIF3(1–100) fusion protein.	Unpublished	Cloning of pHJW183.

Table 4
Oligonucleotides used for the signal-amplifying materials system. The annealing sequences are underlined.

Oligo	Sequence (5'- > 3')
oHJW1	CTTGATCCGGCTGCTAACAAAG
oHJW2	GTGAGCATGGAAACAATACATGGAATC
oHJW3	GAAACAGATTCCATGTATTGTTTCCATGCTCACAAAAGAACTCTATTTTTATTCTGGCGGCGGCAGCG
oHJW4	CTTTGTTAGCAGCCGGATCAAGCTTTTATTAATGATGATGATGATGATGGTGGAATTCACCGGTACGCGTA-GAAC
oHJW5	CTTTGATCTTTTCTACGGGGTCTG
oHJW6	GCGTCAGACCCCGTAGAAAAG
oHJW7	GAGACCACAACGGTTTCCCTC
oHJW8	GTTATCCTCCTCGCCCTTGCTCACGAATTCACCGGTACGCGTAGAAC
oHJW9	GTGAGCAAGGGCGAGGAG
oHJW10	CTTGTACAGCTCGTCCATGCC
oHJW11	ACCGGCGGCATGGACGAGCTGTACAAGTCTGGCGGCGGCAGCG
oHJW12	CTTTGTTAGCAGCCGGATCAAGCTTTTAATGGTGATGGTGATGATGGAATTCACCGGTACGCGTAGAAC
oHJW13	CTAGAGGGAAACCGTTGTGGTC
oHJW14	TCGAGATGCATCATCACCATCACCATCTGGAAGTTCTGTTCCAGGGGCCCTCG
oHJW15	AATTCGAGGGCCCCTGGAACAGAACTTCCAGATGGTGATGGTGATGATGCATC
oHJW136	GACCACAACGGTTTCCCTCTAGAAATAATTTTGTTTAACTTTAAGAAGGAGATATACA-TATGCATCATCACCATCACCATCTG
oHJW141	TGCCATCCACTTCATCGCCA-GAGCCGCCGGATCCGCCGGGTGAACCGCCTCCACCCCGGCGACGACGATTCATG
oHJW142	CTGGCGATGAAGTGGATGGCACCAGCGGCTCTGGCTCTGGCTCTGCTAGCTCGAATTCTTATGACTCCTC-CAGTATC
oHJW143	CATCGCCAGAGCCGCCGGATCCGCCGGGGCCTTCATAGTGGAAGTGGTCTTC
oHJW205	CTCCTTCTTAAAGTTAAACAAAATTATTTCTAGAGG
oHJW421	CTGGAAGTTCTGTTCCAGGGGCCCAGTGGTGTTGATGATGACATGG
oHJW422	CCTGGAACAGAACTTCCAGTGTCTCAATGCCACAGTCCAG
oHJW427	GGATCCGGCGGCTCTGGCATGGTGAGCAAGGGCGAG
oHJW428	CAAATTCGGTATTCGGACCACCAGCAGAACCTGCGG
oHJW429	GGTCCGAATACCGAATTTGCAC
oHJW430	CCAGAGCCGCCGGATCCGCCGGGGCCTTC
oHJW431	GTTTAACTTTAAGAAGGAGATATACATATGCCC
oHJW483	CTGGAAGTTCTGTTCCAGGGGCCCGGTGGAGGCGGTTCAGGAGAGAGCTTGTTTAAGGGGC
oHJW484	CCCTGGAACAGAACTTCCAGGCTAGCAGAGCCAGAGCCAGAGCCGCTGGTGCCATCCACTTCATC
oHJW485	GCGATGAAGTGGATGGCACCAGCGGCTCTGGCTCTGGCTCTGCTAGCCTGGAAGTTCTGTTC-CAGGGGCCCGGTGGAGGCGGTTCATCGAATTCTTATGACTCCTCCAGTATC
oKJ129	CATATGTATATCTCCTTCTTAAAG
oKJ136	CTTTAAGAAGGAGATATACATATGATGGAGAACACTGAAAACTC

2. Experimental design, materials and methods

2.1. Plasmid construction

The cloning details of all plasmids are summarized in Tables 3 and 4.

2.2. Protein production and purification

All proteins were produced in *E. coli* BL21(DE3)pLysS (Invitrogen). The bacteria were cultivated in LB supplemented with ampicillin (100 $\mu g\,mL^{-1}$) and chloramphenicol (36 $mg\,mL^{-1}$) at 37 °C, 150 rpm. Protein production was induced with 1 mM isopropyl β-D-1-thiogalactopyranoside (IPTG) at $OD_{600} = 0.6$. After 4 h at 37 °C, or 30 °C for the TEV constructs, the cells were harvested at 6000 × *g*, 10 min.

The bacterial pellets were resuspended in hydrogel buffer (50 mM NaH_2PO_4, 300 mM NaCl, pH 8.0) supplemented with 10 mM imidazole, and sonicated at 60% amplitude and 0.5 s / 1 s pulse / pause intervals for 10 min on ice. Cellular debris was removed by centrifugation at 30,000 × *g* for 30 min at 4 °C. The proteins in the supernatant were purified by employing Ni-NTA agarose gravity flow columns equilibrated with Ni Lysis buffer. After washing the column twice with 30 mL hydrogel buffer

supplemented with 20 mM imidazole, the proteins were eluted with hydrogel buffer supplemented with 250 mM imidazole. 5 mM 2-mercaptoethanol (2-ME) were added to purified Casp3 and TEV constructs. The buffer of the crosslinking output protein (HJW2) and the 3CPRO inducer (HJW4) was exchanged by dialysis against 5 L hydrogel buffer and usage of SnakeSkin dialysis tubings with 3.5k MWCO (Thermo Fisher). Casp3 was concentrated to 0.5 mL using a Spin-X UF 6 Concentrator (10k MWCO, Corning) at 8,000 × *g*, and applied to a Pierce dextran desalting column (5k MWCO, 5 mL, Thermo Fisher) for the removal of imidazole.

2.3. Synthesis of the materials system

Material A was synthesized by functionalizing epoxy-activated, crosslinked Sepharose 6B (GE Healthcare) with novobiocin as described elsewhere [4] with minor changes.

In brief, the material was reswollen in water for 30 min at RT and washed with 200 mL water per gram epoxy-activated Sepharose. After equilibration with coupling buffer (0.3 M sodium carbonate-bicarbonate buffer, pH 9.5) and addition of 200 mM novobiocin (0.88 mmol novobiocin per gram material) the reaction was incubated at 37 °C for 16 h with shaking. After washing the material with coupling buffer, it was incubated in 1 M ethanolamine, pH 8.5, at 37 °C for 4 h with shaking. After washing with coupling buffer the resulting novobiocin-Sepharose was washed three times with alternate wash steps with water, buffer A (0.1 M Tris/HCl, 0.5 M NaCl, pH 8.0), water, buffer B (0.1 M acetate buffer, 0.5 M NaCl, pH 4.0). The material was blocked with 1% (w/v) bovine serum albumin (BSA) in phosphate-buffered saline (PBS) overnight at 4 °C with agitation.

The binding capacity of the material was analyzed by incubating different amounts of novobiocin-Sepharose with 0.5 nmol GyrB-mEGFP-3CPRO at 4 °C for 7.5 h. The fluorescence in the supernatants was determined at 490/520 nm Ex/Em and correlated to the sample that was incubated without novobiocin-Sepharose (Fig. 6, see section Analytical methods for measurement details). A 6.6-fold excess of GyrB-TEV or GyrB-3CPRO constructs to novobiocin binding sites was used for functionalization in further experiments. After binding at 4 °C overnight, the TEV- and 3CPRO-materials were washed with hydrogel buffer supplemented with 5 mM 2-ME and 0.1% (w/v) BSA. After adding an equal amount of unbound novobiocin-Sepharose the material was incubated for 30 min at RT, and the activities of materials-bound TEV or 3CPRO was determined (see section Analytical methods).

For material B, we synthesized Ni^{2+}-charged poly(acrylamide-co-NTA-acrylamide) as described previously by Ehrbar et al. (see Ref. [5] for synthesis and degree of functionalization of the polymer). For characterization of the polymer, we performed gel permeation chromatography. A stock solution of 3.33 mg mL^{-1} copolymer was prepared in hydrogel buffer supplemented with 300 mM imidazole and 0.05% (w/v) NaN_3. After filtering through a 0.45 μm filter, 0.4 mL of the solution was injected in the GPC device (1260 Infinity LC-System, Agilent). A Suprema three-column system (pre-column, 1000 Å, 30 Å; 5 μm particle size; PSS), which was placed in an external column oven at 55 °C, was used at a constant flow rate of 0.5 mL min^{-1}. A pullulan calibration standard (10 points) served as reference for estimating the average molecular weight (M_n = 439.77 kDa) and polydispersity index (= 1.993).

We synthesized material B by crosslinking 1.8% (w/v) of the polymer with 15 μL output protein (HJW2, 750 μg), optionally supplemented with Casp3 (HJW181). The gels were incubated in humidified atmosphere at RT overnight and transferred to hydrogel buffer supplemented with 5 mM 2-ME. After 6 h, the buffer was exchanged with fresh buffer and the gels were incubated at RT overnight.

The system was assembled by combining TEV-functionalized Sepharose (material A) with one hydrogel (material B) in 1.5 mL hydrogel buffer supplemented with 5 mM 2-ME and 10% (v/v) glycerol. For the assembly of the novobiocin-detection system, 3CPRO-functionalized Sepharose was additionally included. After the addition of inducer (3CPRO or novobiocin), the systems were incubated at RT with agitation. To monitor the system response, supernatant samples were collected at different points in time and stored in polypropylene 96-well plates (Ratiolab) at RT. At the end of each experiment, material B was completely dissolved with 25 mM EDTA. As a measure for the dissolution of material B, the fluorescence of the output mCherry was determined in all samples (see section Analytical methods). EDTA-treated samples served as reference for 100% gel dissolution.

2.4. Analytical methods

Protein concentrations were determined by Bradford assay using Protein assay dye reagent (Bio-Rad). The cleavage and release of proteins from module A was analyzed by subjecting supernatant (S) and total (T, supernatant and material bound protein) protein samples to sodium dodecyl sulfate (SDS) polyacrylamide gel electrophoresis (SDS-PAGE) with 12% (w/v) gels at 160 V. The proteins were subsequently stained with Coomassie brilliant blue and digitized using an ImageQuant LAS 4000 imager (GE Healthcare). mEGFP and mCherry fluorescence were measured in black 96-well plates (Corning) at 490/520 nm or 575/620 nm Ex/Em, respectively, using an Infinite M200 pro microplate reader (Tecan).

TEV activity was determined by using the SensoLyte 520 TEV Activity Kit (AnaSpec). 25 μL TEV sample were mixed with 25 μL substrate in black 96-well plates. The fluorescence was monitored at 490/520 nm Ex/Em and correlated to a dilution series of 5-FAM (0–250 nM 5-FAM in assay buffer, supplemented with TEV substrate, 50 μL per well). 1 RU corresponded to the TEV amount that cleaved substrate equivalent to the fluorescence of 1 pmol 5-FAM per min.

The activity of 3CPRO was determined in transparent 96-well plates (Carl Roth) using the HRV 3C Protease Activity Assay Kit (BioVision). 50 μL 3CPRO sample was mixed with 2.5 μL substrate and the absorbance at 405 nm was monitored in a Multiskan GO Microplate Spectrophotometer (Thermo Fisher). Casp3 activity was determined by activating 15 μg Casp3 (HJW181) with 5 μg 3CPRO (HJW4) in 50 μL hydrogel buffer supplemented with 5 mM 2-ME at RT overnight. The sample was diluted 100-fold and the activity was measured using the Caspase-3 Colorimetric Assay Kit (BioVision). 30 μL Casp3 was mixed with 30 μL assay buffer and 3 μL substrate in transparent 96-well plates. The absorbance at 405 nm was monitored in a Multiskan GO Microplate Spectrophotometer. 1 U Casp3 or 3CPRO corresponded to the amount of protease that cleaved 1 μmol substrate per minute as determined by a *p*-nitroaniline calibration standard.

2.5. Mathematical modeling

A detailed description of the model derivation is described in the Supplementary information in Ref. [1].

2.6. Statistics

Mean values of at least four replicates are shown. Statistical significance of the extended system for novobiocin detection was determined by unpaired t-test with Welch's correction using GraphPad Prism 7; $^{*}p < 0.05$, $^{**}p < 0.01$, $^{***}p < 0.001$.

Acknowledgements

The authors thank Natascha Sprossmann and Frauke Bartels-Burgahn for their technical support. This work was supported by the European Research Council [FP7/2007-2013]/ERC [259043]-CompBioMat and the excellence initiative of the German Federal and State Governments [EXC-294-BIOSS, GSC-4-SGBM].

Transparency document. Supporting information

Transparency data associated with this article can be found in the online version at http://dx.doi.org/10.1016/j.dib.2018.05.074.

References

[1] H.J. Wagner, R. Engesser, K. Ermes, C. Geraths, J. Timmer, W. Weber, *Mater. Today* (in press), 2018.
[2] D.C. Gray, S. Mahrus, J.A. Wells, Cell 142 (2010) 637–646.
[3] D.G. Gibson, L. Young, R. Chuang, J.C. Venter, C.A. Hutchison, H.O. Smith, Nat. Methods 6 (2009) 343–345.
[4] W.L. Staudenbauer, E. Orr, Nucleic Acids Res. 9 (1981) 3589–3603.
[5] M. Ehrbar, R. Schoenmakers, E.H. Christen, M. Fussenegger, W. Weber, Nat. Mater. 7 (2008) 800–804.